

Article

Surrogate Model for Multi-Component Diffusion of Uranium through Opalinus Clay on the Host Rock Scale

Theresa Hennig^{1,2,*}  and Michael Kühn^{1,2} 

¹ GFZ German Research Centre for Geosciences, Fluid Systems Modelling, Telegrafenberg, 14473 Potsdam, Germany; michael.kuehn@gfz-potsdam.de

² Institute of Geosciences, University of Potsdam, Karl-Liebknecht-Str. 24-25, 14476 Potsdam-Golm, Germany

* Correspondence: theresa.hennig@gfz-potsdam.de or thennig@gfz-potsdam.de; Tel.: +49-331-288-28723

Featured Application: Calibration of uranium transport parameters, distribution and effective diffusion coefficient, using multi-component diffusion approach on the core scale, enables reduced complexity models on the host rock scale, simulation speed-up, quantified geochemistry and mineralogy.

Abstract: Multi-component (MC) diffusion simulations enable a process based and more precise approach to calculate transport and sorption compared to the commonly used single-component (SC) models following Fick's law. The MC approach takes into account the interaction of chemical species in the porewater with the diffuse double layer (DDL) adhering clay mineral surfaces. We studied the shaly, sandy and carbonate-rich facies of the Opalinus Clay. High clay contents dominate diffusion and sorption of uranium. The MC simulations show shorter diffusion lengths than the SC models due to anion exclusion from the DDL. This hampers diffusion of the predominant species $CaUO_2(CO_3)_3^{2-}$. On the one side, species concentrations and ionic strengths of the porewater and on the other side surface charge of the clay minerals control the composition and behaviour of the DDL. For some instances, it amplifies the diffusion of uranium. We developed a workflow to transfer computationally intensive MC simulations to SC models via calibrated effective diffusion and distribution coefficients. Simulations for one million years depict maximum uranium diffusion lengths between 10 and 35 m. With respect to the minimum requirement of a thickness of 100 m, the Opalinus Clay seems to be a suitable host rock for nuclear waste repositories.

Keywords: facies; uranium speciation; sorption; reactive transport; heterogeneity; PHREEQC; Mont Terri; repository far-field



Citation: Hennig, T.; Kühn, M. Surrogate Model for Multi-Component Diffusion of Uranium through Opalinus Clay on the Host Rock Scale. *Appl. Sci.* **2021**, *11*, 786. <https://doi.org/10.3390/app11020786>

Received: 27 November 2020

Accepted: 12 January 2021

Published: 15 January 2021

Publisher's Note: MDPI stays neutral with regard to jurisdictional claims in published maps and institutional affiliations.



Copyright: © 2021 by the authors. Licensee MDPI, Basel, Switzerland. This article is an open access article distributed under the terms and conditions of the Creative Commons Attribution (CC BY) license (<https://creativecommons.org/licenses/by/4.0/>).

1. Introduction

For the safe storage of especially highly radioactive waste, emplacement in deep subsurface geological repositories is favoured worldwide to ensure the protection of human and nature from the potential radiation exposure of the waste packages for periods of up to one million years [1]. Claystones are among potential host rocks due to their low permeability. Hence, diffusion is the primary transport process in intact formations [2–4]. Another important and positive aspect of claystones with regard to the storage of nuclear waste is the high sorption capacity retarding the potential migration of radionuclides.

The diffusive transport through the host rock is quantified with numerical simulations usually using Fick's law [2]. According to this method, only one diffusion coefficient is used for all species, major and minor ions as well as all radionuclides, in the same way. A more advanced approach is the multi-component (MC) diffusion, where each species in the system is assigned its own diffusion coefficient and transport is calculated separately for the diffuse double layer (DDL) and the free porewater [5,6]. The surfaces of clay minerals are charged due to their internal structure and contact to the external porewater. Dependent on pH of the solution and the hydroxyl groups on the mineral surface the DDL

forms, compensating the net surface charge by attraction of counter-ions and repulsion of co-ions [7]. Enhanced transport of counter-ions as well as decreased transport of co-ions occurs in the DDL [2,5]. As a consequence, anionic, cationic and neutral species show different diffusive migration pattern in clay formations [6,8].

The Swiss Opalinus Clay is a potential host rock for the storage of nuclear waste [2]. The formation has been investigated for the last 25 years in the underground research laboratory Mont Terri and hence offers a comprehensive database [9]. Furthermore, the MC diffusion approach has already been successfully applied to the Opalinus Clay to model diffusion experiments, for instance with caesium, sodium, chloride and tritium [6]. The Opalinus Clay is subdivided into shaly, sandy and carbonate-rich facies [10], which differ in their mineralogical composition. As a result of the water rock interaction, the geochemical conditions in the porewaters of the facies vary and impact on sorption and transport of radionuclides [11].

Uranium is one of the main components in spent fuel [12], for which we apply diffusion simulations for the far-field (>50 m) of a potential host rock to assess its migration behaviour. Uranium is redox sensitive and its speciation between U(IV) and U(VI) is controlled by the porewater composition. In the geochemical system of the Opalinus Clay, uranium is mainly present as anionic as well as neutral, ternary uranyl complex bound to calcium and carbonate. In a previous study, the migration of uranium in the Opalinus Clay was assessed in one-dimensional diffusion simulations using Fick's laws as a function of different partial pressures of carbon dioxide ($p\text{CO}_2$) covering the range of measured values for the formation and depending on the mineralogical heterogeneity in the facies [11]. The various facies govern the geochemistry of the system, especially via the $p\text{CO}_2$ and thus by the carbonate and calcium concentrations as well as the resulting pH through which the anionic, ternary uranyl complex $\text{CaUO}_2(\text{CO}_3)_3^{2-}$ is the predominant species in the system [11]. Based on their results, Hennig et al. [11] prioritized the governing parameters for the sorption of uranium in the Opalinus Clay as follows: $p\text{CO}_2$, Ca^{2+} concentration, pH, pe and clay mineral quantity. Furthermore, the effect of anion exclusion on the migration lengths was estimated by an adapted porewater diffusion coefficient, what reduced uranium migration by 30%. The work presented here thus aims to extend the findings of Hennig et al. [11] by means of the MC approach.

The first focus in the present study was to assess the deviation between the classical, single-component (SC) and the MC approach in the diffusion lengths of uranium. We know that sorption processes of uranium are facies-dependent [11], hence we investigated and quantified the dependence also for the MC diffusion approach. Many different field and laboratory experiments would be necessary to investigate uranium migration for all geochemical and mineralogical occurrences of the Opalinus Clay. However, those experiments are time-consuming and limited to the metre-scale. In contrast, the safety assessment of a potential nuclear waste repository is required for the host rock scale and for time frames of several hundred thousands of years, what makes numerical simulations indispensable. Unfortunately, MC diffusion on the host rock scale is associated with a huge computational effort. As a second focus, we therefore developed a workflow using MC simulations on the small scale to calibrate transport parameters, which are then used as surrogate of MC diffusion in the SC approach on the host rock scale for simulation times of up to one million years.

2. Methods

For the varying geochemical (Section 2.1) and mineralogical conditions (Section 2.2) in the facies of the Opalinus Clay, one-dimensional diffusion simulations were performed using the MC diffusion approach (Section 2.3) that is implemented in PHREEQC Version 3.5.0 [13].

As first step, we quantified the deviation between the MC approach and the SC method using Fick's law (Section 2.4) by comparing the calculated diffusion lengths on the metre-scale and thus for acceptable computing times. In a second step, we developed a

workflow to calibrate and transfer results of MC diffusion simulations on the metre-scale to the host rock scale (far-field) and a simulation time of one million years. For that, we used a distribution coefficient K_d (m^3/kg) and an effective diffusion coefficient D_e (m^2/s). The K_d was calculated from results of PHREEQC (Section 2.2) and was then used to calibrate the D_e by applying Fick's laws until the results coincide with the MC simulations. The quality of the workflow was evaluated by comparison with a MC simulation.

The underlying thermodynamic data are described in Hennig et al. [11] and updated with the self-diffusion coefficients in water D_w (m^2/s ; Section 2.3, Supplementary Materials S1) for the uranium species [14,15] as well as for the porewater components [13]. All simulations were performed for a temperature of 25 °C in regard to the database. Elevated temperatures as expected due to heat generated by the high-level waste or relevant for greater depths can be neglected, because it is shown that it affects neither the porewater composition (<5% for a temperature of 45 °C) [16] nor the migration behaviour of uranium in the Opalinus Clay up to temperatures of 60 °C [17]. All transport simulations were conducted for hydraulic rock properties corresponding to the direction perpendicular to bedding. The uranium source term from the failed high-level waste canisters is represented by a Dirichlet boundary with a constant uranium concentration of 1 $\mu\text{mol}/\text{L}$ [17,18]. Since our focus lies on the migration behaviour of uranium in the far-field, we do not consider the effect of the engineered barriers on the source term [2], such as a delay and retention due to the metal canisters or the bentonite filling. This constraint is a simplification of the nuclear waste repository concept and hence our results need to be considered as maximum diffusion lengths. Neumann boundary is applied to the model outlet.

2.1. Geochemical System of the Opalinus Clay

The facies of the Opalinus Clay are defined in the simulations based on mineralogical and geochemical data from bore hole logs at Mont Terri (Table 1). The concentrations of the main ions in the porewater are averaged for the measurement series and electro neutrality of the solution ($\pm 3\%$) is established via chloride [11]. The composition of the porewater stems from marine origin and the interaction with the minerals, such as cation exchange and/or dissolution as well as precipitation [10,19]. Due to the geological age of the formation and the associated contact time between minerals and porewater, thermodynamic equilibrium between both is assumed [10,19–21].

The speciation of uranium in the porewater and its sorption on the Opalinus Clay highly depends on the pCO_2 [11] as it controls the concentrations of carbonates and calcium as well as pH in solution [10,19]. Measurements of pCO_2 in the Opalinus Clay are associated with a degree of uncertainty [10,22,23] and we therefore decided to fix it to $10^{-2.2}$ bar as recommended for clay formations with similar mineral assemblages [10,21,24]. Depending on pCO_2 , the porewaters of the facies are equilibrated with the carbonates calcite, dolomite and siderite to control pH and the concentrations of calcium, magnesium and iron [25]. For the applied pCO_2 of $10^{-2.2}$ bar, uranium is mainly present as anionic, ternary uranyl complex $\text{CaUO}_2(\text{CO}_3)_3^{2-}$ in the porewater [11]. For in-situ conditions, porewater in the Opalinus Clay is moderately reducing [21,23]. An initial E_H of -227 mV published by Bossart and Thury [26] was chosen and governed in the simulations via an equilibrium with the minerals pyrite and siderite. These minerals, or the redox couple $\text{SO}_4^{2-}/\text{HS}^-$, provide the most consistent results with measurements [10,19,21,23].

2.2. Integrating Sorption Processes

The varying mineralogy of the Opalinus Clay is implemented in the simulations with a bottom-up approach [27,28]. The amount of sorption of contaminants in heterogeneous formations can be determined by the additive sorption on individual minerals. It is quantified with mechanistic surface complexation models (SCM) using the two-layer model of Dzombak and Morel [29] and cation exchange [30]. The respective and proven SCM dataset [31] with all surface parameters and reactions is given in the Supplementary Materials of Hennig et al. [11]. We only consider sorption on the main clay minerals

illite, illite/smectite mixed layers, kaolinite and chlorite (Scenario MC_{4Clay}) as the contribution of the other minerals to the total sorption can be neglected (<1%) [11]. The illite/smectite mixed layers are handled as a combination of the pure clay minerals (illite and smectite) with a proportion of 1:1 [31]. Smectite is a generic term for a group of clay minerals and not further described for the Opalinus Clay. We decided to use montmorillonite as representative because it is the best investigated [31]. Cation exchange is considered for the main cations and uranyl-ions on illite and montmorillonite as exchange phases [11]. The respective reactions are given as well in the Supplementary Materials of Hennig et al. [11]. The distribution coefficient K_d (m³/kg) is defined by the ratio between the amount of a species adsorbed on the solid phase and the amount present in the liquid phase. The K_d is calculated in PHREEQC for each facies depending on the geochemical and mineralogical conditions following Stockmann et al. [28]. In the literature, sorption of uranium on Opalinus Clay is commonly modeled using only the clay minerals illite and montmorillonite [32–35]. We followed that approach and assessed the effect of various mineral compositions on the resulting diffusion length (Scenario MC_{2Clay}).

Table 1. Input parameters representing the three facies, shaly, sandy and carbonate-rich. Concentrations are given as average values from the borehole analyses. Shaly-76 and Shaly-61 correspond to the clay mineral content in wt.% at the sampled location.

Parameter	Unit	Shaly-76 ^{a,b}	Shaly-61 ^{c,d}	Sandy ^{e,f}	Carb-Rich ^{g,h}
pH	-	7.13	7.50	7.40	7.28
Na ⁺	mmol/L	281	230	121	195
K ⁺	mmol/L	1.93	1.47	0.87	0.73
Mg ²⁺	mmol/L	21.97	16.79	5.91	15.89
Ca ²⁺	mmol/L	18.90	16.03	6.73	16.37
Sr ²⁺	mmol/L	0.46	0.47	0.35	0.44
Fe _{total}	μmol/L	29.62	8.37 ^d	9.81 ^f	9.81 ^f
U _{total}	nmol/L	2.28 ^d	2.28 ^d	2.52 ^f	2.52 ^f
Cl ⁻	mmol/L	327	273	121	242
SO ₄ ²⁻	mmol/L	16.79	12.30	6.94	16.03
PO ₄ ³⁻	μmol/L	21.65 ^d	21.65 ^d	10.65 ^f	10.65 ^f
Alkalinity	mmol/L	3.85	1.24	2.61	2.05
I ⁱ	mol/L	0.38	0.32	0.16	0.28
DDL ^j	nm	0.49	0.54	0.76	0.57
Illite	wt.%	20	17	17	8
IS mixed ^k	wt.%	16	12	8	6
Kaolinite	wt.%	30	26	13	8
Chlorite	wt.%	10	6	7	4
ΣClay	wt.%	76	61	45	26
Calcite	wt.%	14	11	17	42
Dolomite	wt.%	n.a.	2	2	3
Siderite	wt.%	1	4	2	2
Porosity ϵ	-	0.166 ^l	0.162	0.137 ^m	0.155
wet water content $w_{C_{wet}}$	-	0.068 ^l	0.070	0.055 ^m	0.063
dry bulk density ρ_{db}	kg/m ³	2290 ^l	2280	2365 ^m	2320
wet bulk density ρ_{wb}	kg/m ³	2458 ^l	2456	2498 ^m	2480

n.a., no data available; ^a [22], borehole BPC-C1; ^b [10], borehole BPP-1; ^c [19], borehole BWS-A1; ^d [10], borehole BWS-A1; ^e [19], borehole BWS-A3; ^f [10], borehole BWS-A3; ^g [10], borehole BGP-1; ^h [10], borehole EPFL; ⁱ calculated in PHREEQC, pCO₂ = 10^{-2.2} bar; ^j Thickness Donnan-layer, calculated via ionic strength [36]; ^k IS mixed, illite/smectite mixed layers; ^l [10], borehole BWS-A6; ^m [10], borehole BWS-E3.

Porosity, bulk density and water content vary for each facies [10]. These parameters influence the simulation results as they define the amount of porewater per volume unit Opalinus Clay and the amount of clay minerals per kilogram porewater. Therefore, we performed various scenarios of MC diffusion simulations for the minimum and maximum

amount of rock per kilogram porewater (Scenarios MC_{min} and MC_{max} , Table 2) as well as with different clay mineral compositions (Scenarios MC_{4Clay} and MC_{2Clay}).

Table 2. Porosity (ϵ), dry and wet bulk density (ρ_{db} and ρ_{wb}) as well as wet water content (wc_{wet}) used for the scenarios with the minimum and maximum amount of rock per kilogram porewater for the facies of the Opalinus Clay [10].

Parameter	Shaly-76		Shaly-61		Sandy		Carb-Rich	
	Min	Max	Min	Max	Min	Max	Min	Max
Porosity ϵ (-)	0.191	0.141	0.191	0.141	0.177	0.130	0.171	0.155
wet water content wc_{wet} (-)	0.051	0.086	0.051	0.086	0.053	0.078	0.053	0.075
dry bulk density ρ_{db} (kg/m ³)	2230	2410	2230	2410	2260	2400	2280	2400
wet bulk density ρ_{wb} (kg/m ³)	2420	2530	2420	2530	2440	2530	2450	2530
Rock per kg porewater (kg _{rock} /kg _{pw})	11.55	16.95	11.55	16.95	12.36	18.17	13.20	15.24

2.3. Modelling Multi-Component Diffusion

In contrast to Fick's laws, the transport of species in the MC diffusion approach is not based on a concentration gradient but on the electrochemical potential μ [5,6,13,37,38]:

$$\mu = \mu^0 + RT \ln \alpha + zF\psi \quad (1)$$

with μ^0 the standard potential (J/mol), R the gas constant (8.314 J K⁻¹ mol⁻¹), T the absolute temperature (K), α the activity (-), z the charge number (-), F the Faraday constant (96,485 J V⁻¹ eq⁻¹) and ψ the electrical potential of a charged surface (V). This enables calculation of the diffusive flux in uncharged (free porewater) and charged regions (DDL) of the clay minerals or the interlayer space between the clay layers. Appelo et al. [6] successfully applied the approach for the Opalinus Clay to model a diffusion experiment with neutral, cationic and anionic species. Furthermore, it was used to obtain the porewater composition in the Callovo-Oxfordian clay rock [37].

The diffusive flux of a species in solution J_i (mol m⁻² s⁻¹) as result of the chemical and electrical potential gradients becomes [5,6,13,38]:

$$J_i = -\frac{u_i c_i}{|z_i| F} \frac{\partial \mu_i}{\partial x} - \frac{u_i z_i c_i}{|z_i|} \frac{\partial \psi}{\partial x} \quad (2)$$

with u_i the mobility in water (m² s⁻¹ V⁻¹), c_i as species concentration in the accessible porewater (mol/m³) and x as spatial coordinate (m). The mobility in Equation (2) is related to the tracer diffusion coefficient in water $D_{w,i}$ (m²/s):

$$u_i = D_{w,i} \cdot \frac{|z_i| F}{RT} \quad (3)$$

Due to the different transport velocities of ions, a charge with an associated potential is created and thus the gradient of the electrical potential ($\partial\psi/\partial x$) in Equation (2). The electrical potential in Equation (1) stems from a charged surface and is therefore fixed without inducing any electrical current. Accordingly, both potentials may differ from each other [5,6,13,38]. If there is no electrical current, $\sum z_i J_i = 0$. This zero-charge flux condition allows to eliminate the electrical potential gradient ($\partial\psi/\partial x$) from Equation (2) by expressing it as a function of the other terms in Equation (2) [5,6,13,38]. Any charge imbalance that may for instance exist in the DDL is maintained by the zero-charge flux condition and hence the equation is also valid, if the solution is not electrically neutral.

Within PHREEQC, the diffusive flux for every species present in the system is calculated as the sum of the transport in the porewater as well as in the DDL for the MC option. Conceptually, the porous medium within a model element is subdivided along its length in paired cells for each mineral present (Figure 1). Accordingly, each pair of cells consists of a charge-balanced solution, the free porewater, and a charged surface with a DDL. In the case of negatively charged surfaces, cations are enriched in the DDL to compensate

the remaining net surface charge and anions are excluded. Consequently, the pore space accessible for anions is reduced and so their diffusive flux. This is known as the anion exclusion effect. In the simulations, anion exclusion is controlled by the composition and amount of water in the DDL. The composition of the DDL is calculated as average using the fast and robust method of the Donnan approximation implemented in PHREEQC [13], which assumes a single potential for the DDL as an entity [5]:

$$c_{i,DDL} = c_i \cdot \exp\left(\frac{-z_i F \psi_{DDL}}{RT}\right) \tag{4}$$

with $c_{i,DDL}$ the concentration of species i in the Donnan pore space (mol/m^3) and ψ_{DDL} the potential in the DDL (V) to ensure zero charge of the paired cells. The potential ψ_{DDL} of the Donnan volume is adapted to counterbalance the surface charge [13]. Hence, the concentrations in the DDL are linked to the concentrations in the free porewater c_i (mol/m^3) and the surface charge that must be neutralized [39]. The thickness of the DDL is determined via the ionic strengths (Table 1) [36]. MC diffusive transport in a model element is calculated by explicit finite differences for each interface among the cells and summed up for the diffusive transport between two model elements. A more detailed description of the approach can be found in Appelo and Wersin [5], Appelo [38] and Appelo et al. [6].

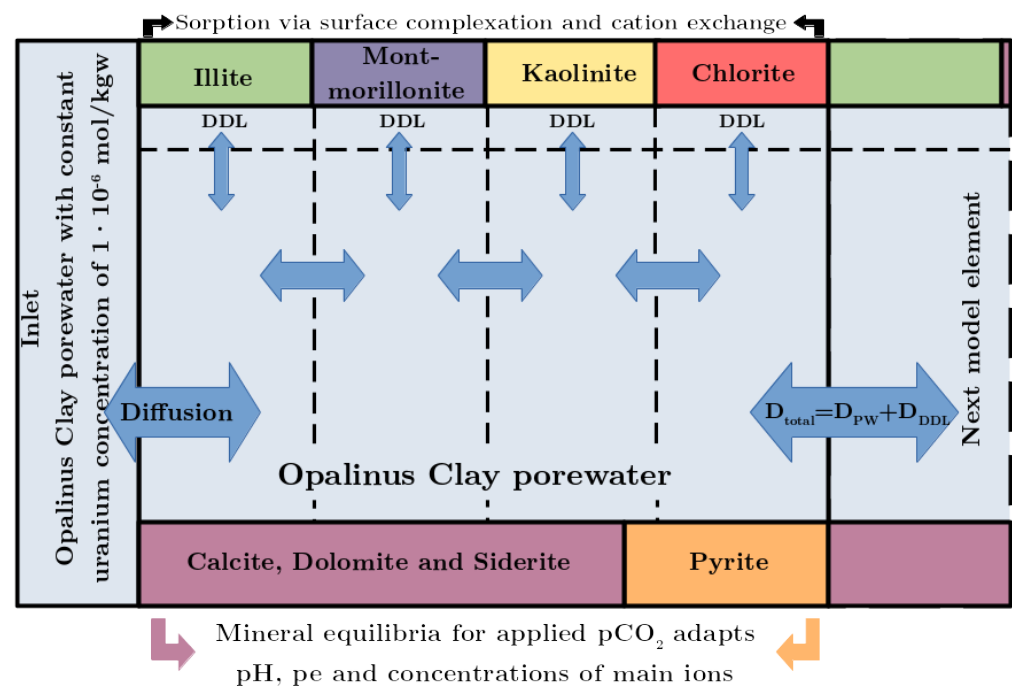


Figure 1. Concept of the one-dimensional finite-difference diffusion model in PHREEQC.

In porous media, diffusive transport is impeded by tortuosity of the pores, the reduced cross-sectional area available for diffusion and the pore sizes [40], which is reflected by the effective diffusion coefficient D_e (m^2/s). PHREEQC assumes that a model element exclusively contains water [13] and therefore the pore water diffusion coefficient D_p (m^2/s) is applied instead to calculate the diffusive flux. Equation (5) gives the relation between D_p and D_e . In PHREEQC, D_p is derived analogous to Archie’s law via the self-diffusion coefficient in water D_w (m^2/s), the accessible porosity ϵ (-) and an empirical exponent n (-):

$$D_e = D_p \cdot \epsilon = D_w \cdot \epsilon^n \tag{5}$$

The empirical exponent n is a constant, medium-specific parameter [41] and needs to be determined for the Opalinus Clay (Section 3) to use the MC approach in PHREEQC. In order to individually calculate the diffusive flux for each species present in the system, D_w

must be assigned in the database. The D_w of all relevant uranyl species were calculated by molecular-dynamic simulations and are taken from Kerisit and Liu [14] as well as from Liu et al. [15]. In the case of a missing D_w for an uranium species, the diffusion coefficient of a chemically similar one was chosen to be used instead. All other necessary self-diffusion coefficients stem from the database `phreeqc.dat` provided with PHREEQC [13]. The selected D_w are given in the Supplementary Materials S1.

On the metre-scale, MC simulations were performed for each facies (Table 1, Section 2.1) as well as for varying mineral quantities and compositions (Table 2, Section 2.2) for models of 1 m with a spatial resolution of 0.01 m and a simulation time of 100 years. Simulations on the host rock scale were conducted for each facies with a model of 50 m and a spatial resolution of 0.5 m and a simulation time of one million years. Grid independence of the diffusion models on both scales was confirmed by simulations with finer resolutions.

2.4. Modelling Single-Component Diffusion

The classical SC diffusion simulations were conducted in Python-based diffusion models for each facies using Fick's laws and finite-differences. The spatial resolution is 0.005 m on the small scale (1 m) and 0.25 m on the far-field scale (50 m) to ensure grid independence. Sorption is considered via the distribution coefficient K_d calculated for every facies in the MC simulation, as described in Section 2.2. Since only one diffusion experiment with uranium in Opalinus Clay of the sandy facies is given in the literature [17], this effective diffusion coefficient is used for all facies in the SC simulations. The D_e was determined in the experiment for a temperature of 25 °C and perpendicular to bedding with $1.9 \times 10^{-12} \text{ m}^2/\text{s}$ [17]. Porosities are taken from Table 1.

3. Model Calibration

The medium-specific parameter n required for the MC diffusion approach to determine the effective diffusion coefficient for every species (Equation (5)) was calibrated using an experiment with U(VI) and Opalinus Clay of the sandy facies [17]. We set up a model equal to the one presented in Hennig et al. [11] with the additional application of the MC diffusion approach. For the diffusion experiment, the precise composition of the minerals was not determined. Therefore, the mineral composition used here is based on the results given in Hennig et al. [11] (23 wt.% kaolinite, 9 wt.% illite, 4 wt.% illite/smectite mixed layers and 9 wt.% chlorite) for a clay mineral content of 45 wt.% corresponding to the sandy facies [10]. The parameter n was varied until the best coincidence between the MC diffusion simulations and the experimental data was achieved. For the simulations considering sorption on all clay minerals ($\text{MC}_{4\text{Clay}}$, illite, montmorillonite, chlorite and kaolinite), an exponent n of 2.6 was determined, whereas for the model concept with only two clay minerals ($\text{MC}_{2\text{Clay}}$, illite and montmorillonite) the best match between experimental and modeled data was observed for an n of 2.1. Both results and the experimental data are shown in Figure 2.

In the literature, values for the medium-specific parameter n of 2.4 [42] and 2.5 [4,43,44] are given for Opalinus Clay, which is in line with the value $n = 2.6$ of our $\text{MC}_{4\text{Clay}}$ concept. For bentonite mainly consisting of montmorillonite, a value of $n = 1.9$ can be found [45], which is similar to the $\text{MC}_{2\text{Clay}}$ concept with only illite and montmorillonite as clay minerals and an exponent $n = 2.1$. However, the experimental data can be reproduced as shown in Figure 2. The relative Root Mean Square Errors (rRMSE) are calculated in relation to the experimental data. The values for the rRMSE are 28% for an $n = 2.6$ ($\text{MC}_{4\text{Clay}}$) and 27% for an $n = 2.1$ ($\text{MC}_{2\text{Clay}}$). Due to the scattering of the data, we consider our model concepts for the exponents $n = 2.6$ ($\text{MC}_{4\text{Clay}}$) and $n = 2.1$ ($\text{MC}_{2\text{Clay}}$) as best fit and calibrated for further application.

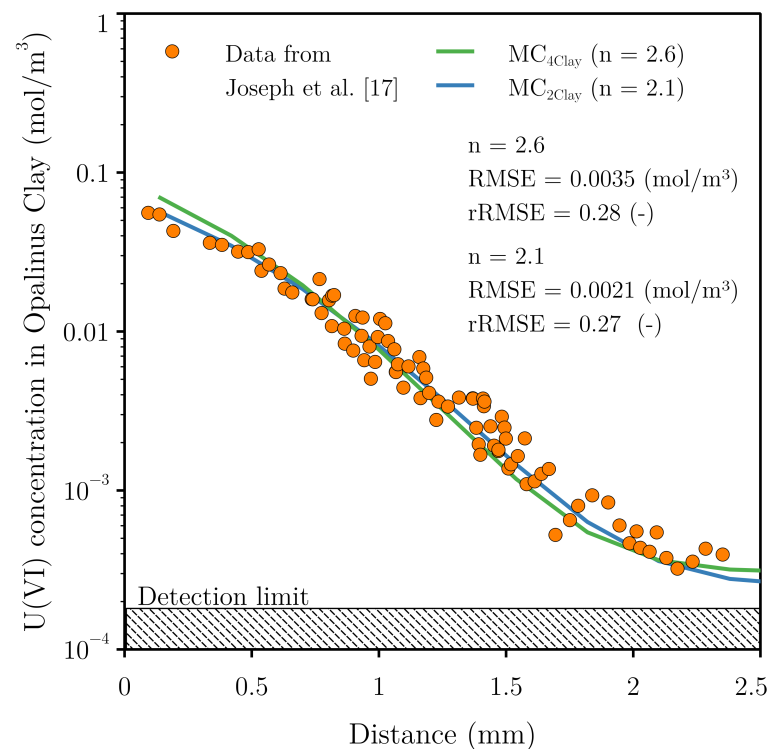


Figure 2. For the model concept considering all clay minerals (kaolinite, illite, montmorillonite and chlorite) for sorption (MC_{4Clay} , green line), the modeled results match with the experimental data (dots) of the diffusion experiment with U(VI) and Opalinus Clay of the sandy facies for an exponent n of 2.6. For the model taking into account only the two clay minerals illite and montmorillonite (MC_{2Clay} , blue line), n is 2.1.

4. Results

4.1. Multi- and Single-Component Simulations on the Metre-Scale

The difference between MC and SC diffusion was determined depending on mineralogical and geochemical variations in the facies of the Opalinus Clay (Table 1) by quantifying and comparing the resulting migration lengths of uranium. MC diffusion simulations were performed for two model concepts (MC_{4Clay} and MC_{2Clay}), which differ in the clay minerals considered for sorption, to identify the effect of the clay mineral composition on the migration lengths. For all facies, the results of the MC simulations for the two model concepts as well as the SC simulations are shown in Figure 3.

Differences in the migration length between the MC and SC approach are obvious in all facies. After a simulation time of 100 years, the maximum diffusion lengths determined with the MC diffusion approach ranged from 0.12 m in the shaly (MC_{4Clay} , Figure 3a) up to 0.24 m in the sandy facies (MC_{4Clay} , Figure 3d). Using the SC diffusion approach, the migration lengths varied between 0.14 m in the shaly (Figure 3a) and 0.23 m in the carbonate-rich facies (Figure 3b). In the shaly and carbonate-rich facies, uranium migrated less far into the Opalinus Clay in the MC simulations compared to SC, whereas, in the sandy facies, it was opposite. The difference in migration length in a facies between the two approaches varied from around 0.07 m less (Figure 3b) up to 0.02 m farther (Figure 3d) into the formation using the MC approach with four clay minerals (MC_{4Clay}).

Consideration of only two (MC_{2Clay}) instead of four clay minerals (MC_{4Clay}) for sorption in the MC simulations led to a farther migration of uranium into the model and thus reduced the difference between MC and SC in the shaly (Shaly-76) as well as carbonate-rich facies (Figure 3a,c). However, uranium still migrated less far into the Opalinus Clay compared to the SC approach. For the second mineral composition representing the shaly facies (Shaly-61), uranium migration was roughly 0.01 m less far into the formation, when using only two clay minerals (MC_{2Clay} , Figure 3c). In the sandy facies, the migration

lengths changed from 0.02 m farther to 0.08 m less into the formation in the MC simulations compared to the SC (Figure 3d).

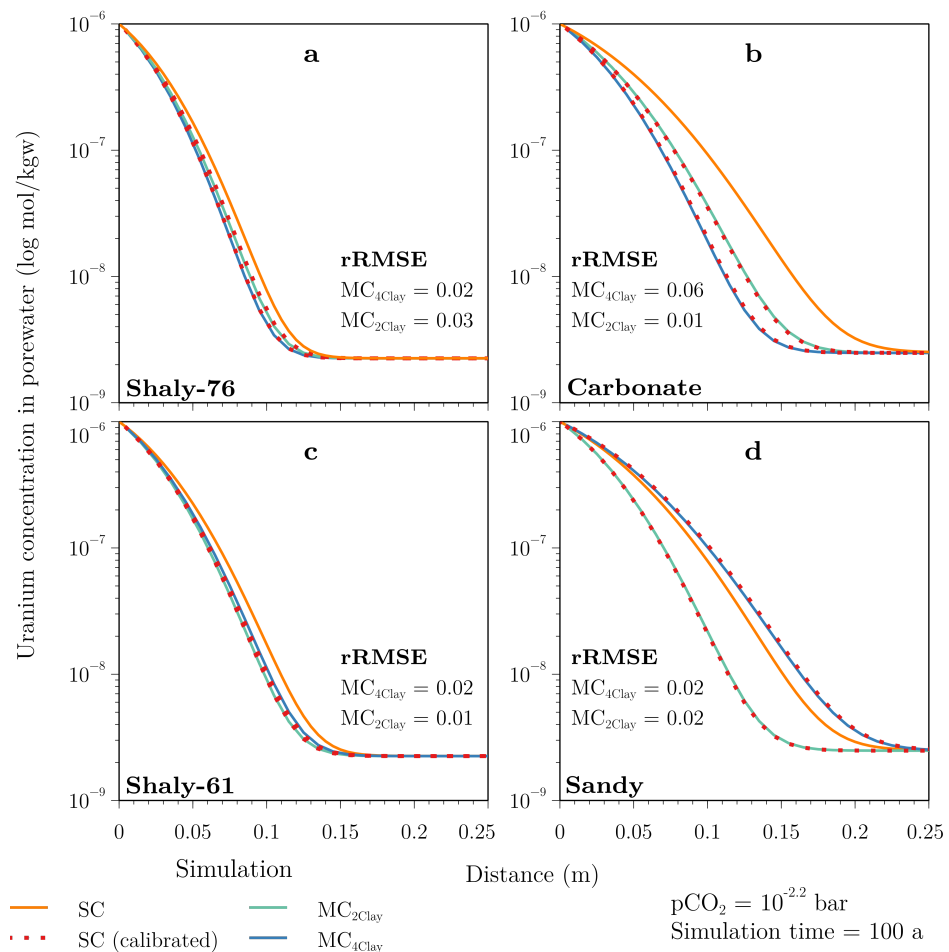


Figure 3. Concentration of uranium in the porewater of the shaly (a,c), carbonate-rich (b) and sandy facies (d) for the MC diffusion (MC_{2Clay}, light blue line, and MC_{4Clay}, dark blue line) as well as the SC approach (SC, orange line). The red, dotted lines represent the results of the simulations based on the SC approach using the K_d and D_e calibrated from the MC simulations. The rRMSE indicates the deviation between the simulations with the calibrated parameters and the respective MC simulation. The number behind the shaly facies corresponds to the clay mineral content in wt.%.

The results of the MC simulations could be reproduced with the SC approach using the calculated K_d and calibrated D_e given in Table 3 with a deviation between 1% and 6% (average 2%) between the calibrated SC and the MC simulations. In the experiment, a K_d of $0.025 \text{ m}^3/\text{kg}$ was identified [17]. All of our calculated K_d values are an order of magnitude smaller and decrease with the clay mineral content, with only a minimal difference in sorption between the sandy and carbonate-rich facies despite the fact that 20 wt.% more clay minerals are in the sandy facies (Table 3). It is to be highlighted that the K_d values (Table 3) of the shaly facies are more than twice as large compared to the sandy and carbonate-rich facies. For all facies, the K_d values and hence sorption were slightly reduced using the MC_{2Clay} scenario. The calibrated D_e range from $1 \times 10^{-12} \text{ m}^2/\text{s}$ to $2.25 \times 10^{-12} \text{ m}^2/\text{s}$ (Table 3) for the MC_{4Clay} scenario and thus the experimentally determined value of $1.9 \times 10^{-12} \text{ m}^2/\text{s}$ from the diffusion experiment of Joseph et al. [17] is within our range. The MC_{2Clay} scenario only slightly increases the effective diffusion coefficients for the carbonate-rich facies, whereas in the sandy and shaly facies (Shaly-61) it leads to a reduction. For the location with the highest clay mineral content (Shaly-76), the D_e is equal for both scenarios.

Table 3. Calibrated transport parameters (K_d and D_e) from the different scenarios of the MC diffusion simulations on the metre-scale and after a simulation time of 100 years for the facies of the Opalinus Clay.

Scenario	Parameter	Shaly-76	Shaly-61	Sandy	Carb-Rich
MC _{4Clay}	K_d (10^{-3} m ³ /kg)	4.04	3.09	1.55	1.43
	D_e (10^{-12} m ² /s)	1.50	1.60	2.25	1.00
MC _{max}	K_d (10^{-3} m ³ /kg)	4.04	3.09	1.55	1.43
	D_e (10^{-12} m ² /s)	1.00	1.10	2.00	1.00
MC _{min}	K_d (10^{-3} m ³ /kg)	4.04	3.09	1.55	1.43
	D_e (10^{-12} m ² /s)	2.20	2.65	4.50	1.25
MC _{2Clay}	K_d (10^{-3} m ³ /kg)	3.64	2.71	1.10	1.29
	D_e (10^{-12} m ² /s)	1.50	1.40	0.80	1.15

The composition of the DDL was calculated for each clay mineral dependent on the geochemical conditions in a facies using the Donnan approximation implemented in PHREEQC. The total amount of water in the DDL is distributed mainly via illite (72–79%) and montmorillonite (15–20%), followed by kaolinite (5–9%) and chlorite (0.3–0.5%) as a result of the geochemical conditions and mineral composition. The concentrations in the DDL of the clay minerals are shown in Figure 4 for calcium and magnesium (Figure 4a), sulphate and chloride (Figure 4b,c) and uranium (Figure 4d). As the distribution of the different species across the DDL differs only in absolute numbers, we decided to give the results exemplary only for the sandy facies. The highest uranium concentration across the DDL was observed in chlorite (Figure 4d). This also applied to sulphate (Figure 4b), except for the sample Shaly-76. For this mineral composition, the highest sulphate concentrations were found in the DDL of illite. The other ions, such as chloride, calcium or magnesium, were mainly located in the DDL of illite (Figure 4a,b). The concentrations of uranium, magnesium and calcium in the DDL of chlorite decreased along the x-axis, while the sulphate and chloride concentrations simultaneously increased (Figure 4).

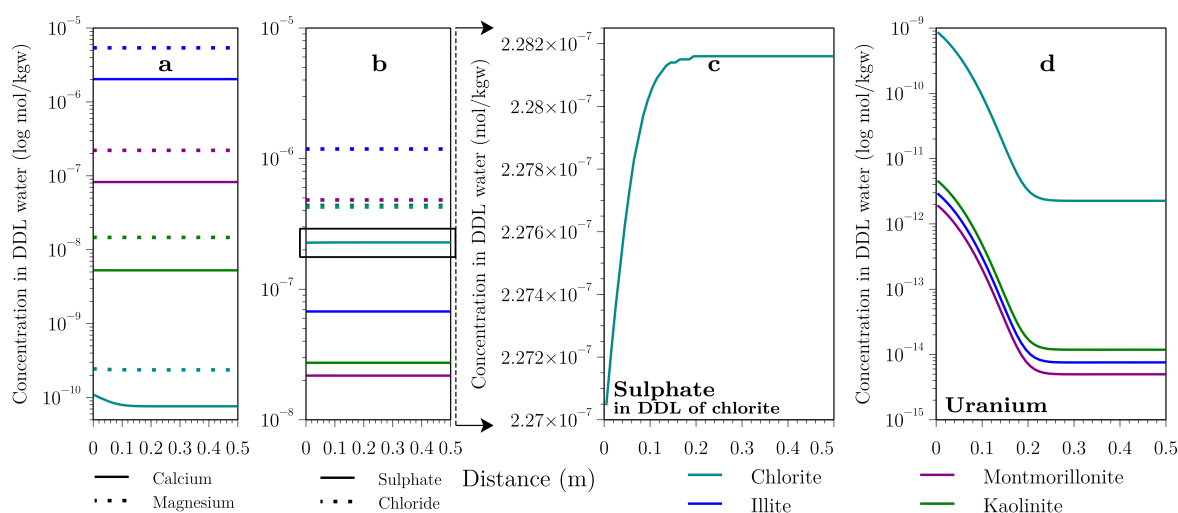


Figure 4. Concentrations of calcium and magnesium (a), sulphate and chloride (b,c) and uranium (d) in the DDL of the clay minerals for the sandy facies after a simulation time of 100 years and for a $p\text{CO}_2$ of $10^{-2.2}$ bar. For better clarity, the concentration of sulphate in the DDL of chlorite is given in c as close-up of (b).

4.2. Multi-Component Diffusion for Varying Total Amounts of Minerals on the Metre-Scale

The migration of uranium as a function of the variability of hydro-physical parameters, e.g., porosity or dry bulk density, and the resulting amounts of minerals within a facies of the Opalinus Clay were simulated in minimum and maximum scenarios (MC_{max} and

MC_{min} , Table 2) using MC diffusion simulations (MC_{4Clay}) on the metre-scale. The effect of the total mineral amount on the diffusion lengths was quantified by comparison with the MC simulations based on the averaged data given in Table 1. From the results of the MC simulations, K_d was calculated and D_e calibrated to reproduce the MC simulations with the SC approach. Figure 5 shows the results of the MC simulations for the minimum and maximum total amount of rock for all facies as well as the SC simulations using the calibrated transport parameters.

In all facies, uranium migrated farther into the formation for the MC_{min} scenario. After a simulation time of 100 years, the maximum diffusion length of 0.35 m was determined in the sandy facies (Figure 5d). The difference in migration distance between the two scenarios for the total amount of rock per kg porewater ranged from 0.02 m in the carbonate-rich facies (Figure 5b) to 0.13 m in the sandy facies (Figure 5d). In Figure 5b,d, the diffusion lengths of the maximum scenarios are similar to the simulations using the averaged values of the hydro-physical parameters. For all scenarios and facies, MC simulations could be reproduced with the calibrated transport parameters with a deviation between 1% and 6% (average 3%) between SC and MC simulation (Figure 5).

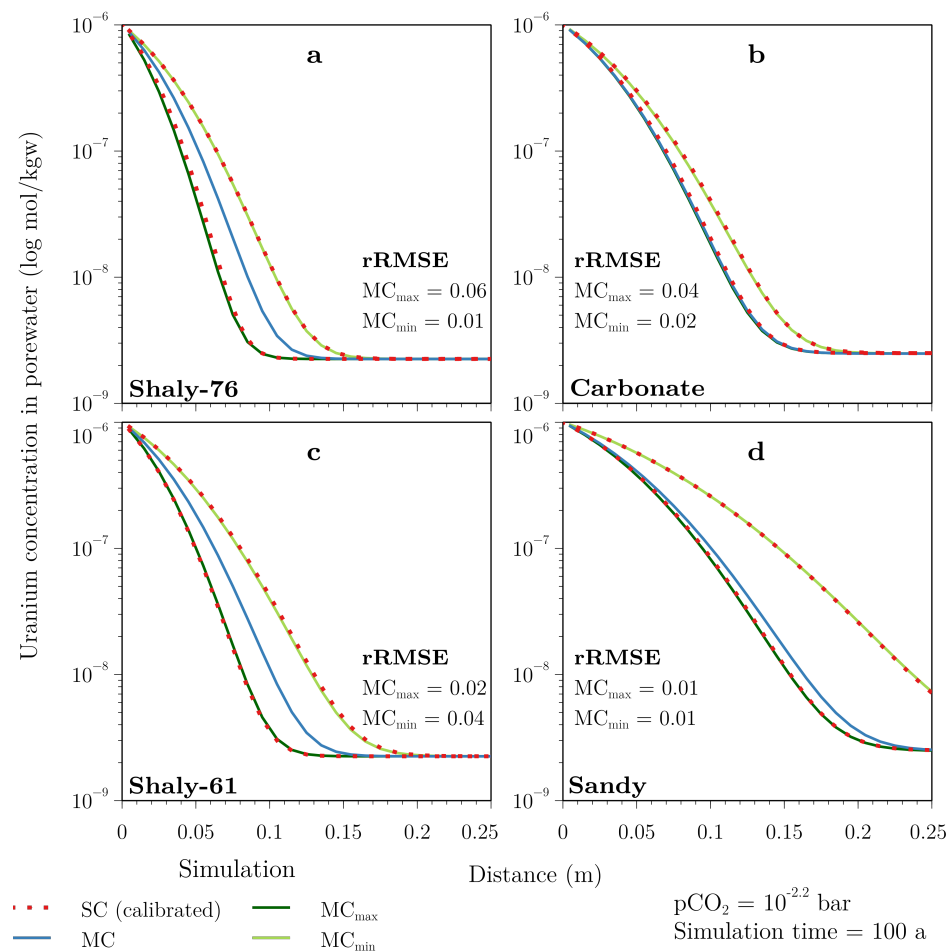


Figure 5. Concentration of uranium in the porewater of the shaly (a,c), carbonate-rich (b) and sandy facies (d) for the scenarios with minimum (MC_{min} , 12–13 kg_{rock}/kg_{pw} , light, green line), maximum (MC_{max} , 15–18 kg_{rock}/kg_{pw} , dark, green line) and average (MC, 14–17 kg_{rock}/kg_{pw} , blue line) total amount of rock per kg porewater. The red, dotted lines represent the results of the simulations based on the SC approach with the K_d and D_e calibrated from the MC simulations.

The K_d and D_e for the scenarios presented in Figure 5 are given in Table 3. The calculated K_d values are unaffected by the variation in total mineral amount, whereas especially the calibrated D_e of the MC_{min} more than doubles in some cases compared to

the value of 1.9×10^{-12} (m²/s) determined in the diffusion experiment of Joseph et al. [17]. The D_e of all scenarios showed the least variation from each other in the carbonate-rich and the highest in the sandy facies.

4.3. Transfer of Multi-Component Diffusion Simulations to the Host Rock Scale

The applicability of K_d and D_e calibrated from the 1 m-model to the host rock scale (50 m) was evaluated by comparison with a MC simulation (MC_{4Clay}). The other scenarios (MC_{max} , MC_{min} and MC_{2Clay}) were calculated using the SC approach and the calibrated parameters given in Table 3 to quantify the influence of the mineral composition and total amount on the host rock scale. All results on the host rock scale are shown in Figure 6.

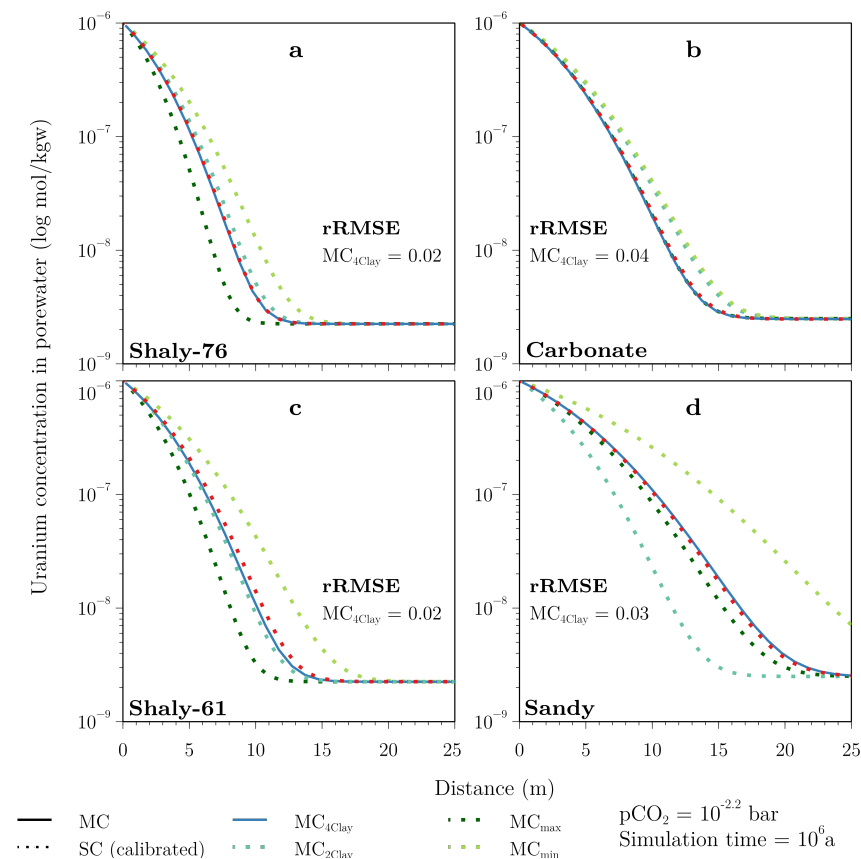


Figure 6. Concentration of uranium in the porewater of the shaly (a,c), carbonate-rich (b) and sandy facies (d) for the scenarios with minimum (MC_{min} , light, green line), maximum (MC_{max} , dark, green line) and average (MC, blue line) total amount of rock per kg porewater as well as for the concepts considering four (MC_{4Clay}) and two clay minerals (MC_{2Clay}) for sorption. Dotted lines mean that the SC approach with the calibrated K_d and D_e was used, with red representing the results for the MC_{4Clay} scenario for better visibility. Only MC_{4Clay} (blue line) is based on the MC diffusion approach.

After a simulation time of one million years, diffusion lengths of uranium for the MC_{4Clay} scenario varied in the facies between 13 m (Figure 6a) and 24 m (Figure 6d). For all facies, the MC simulations could be reproduced on the host rock scale with the K_d and D_e calibrated on the small scale with an average deviation of 3% (MC_{4Clay} and rRMSE, Figure 6). Considering two (MC_{2Clay}) or four (MC_{4Clay}) clay minerals for sorption did not significantly influence the migration of uranium in the shaly and carbonate-rich facies (Figure 6a–c), whereas, in the sandy facies, it reduced uranium migration by 8 m, from 24 m (MC_{4Clay} , Figure 6d) to 16 m (MC_{2Clay} , Figure 6d). The scenarios for the minimum and maximum total amount of minerals per kg porewater led to differences in the diffusion lengths between 2 m (Figure 6b) and 13 m (Figure 6d). Depending on the total amount

of rock, maximum diffusion lengths of uranium ranged from 10 m in the shaly (MC_{max} , Figure 6a) to 35 m in the sandy facies (MC_{min} , Figure 6d).

The computing times for the individual scenarios in Table 3 varied on the metre-scale between 1 h and 2 h for the MC approach and a few seconds for the SC calculations. On the host rock scale, the MC simulations required a computing time between 5 h and 6 h ($6\text{ h} = 21,600\text{ s}$), whereas the SC simulations were done in a few seconds ($<10\text{ s}$). This provides a time saving of four orders of magnitude (factor of 2×10^4).

5. Discussion

From the study of Hennig et al. [11], we know that sorption processes and thus migration of uranium in the Opalinus Clay are controlled by the calcite-carbonate system. The authors identified the governing parameters in descending priority as follows: pCO_2 , Ca^{2+} concentration, pH, pe and the amount of clay minerals. Hence, geochemistry is more decisive for uranium sorption than the clay mineral content, whereby its influence increases with decreasing amount of clay minerals. This, in turn, results in a facies-dependence of uranium sorption as the heterogeneous mineralogy in the facies leads to differences in the composition of the porewater as a result of water rock interactions. As our geochemical system is identical to the one of Hennig et al. [11], these findings are also valid here. Furthermore, Hennig et al. [11] estimated that anion exclusion reduces the diffusion lengths of uranium by 30%.

5.1. Differences between Single- and Multi-Component Diffusion Approach

Based on the migration lengths of uranium, differences between the SC and MC diffusion approach were quantified on the metre-scale. For the MC_{4Clay} concept, uranium migrated less far into the model for all facies using the MC approach except for the sandy facies, where it migrated farther (MC_{4Clay} , Figure 3). We presume that not only sorption processes of uranium are facies-dependent in the Opalinus Clay [11], but also the diffusive transport. The difference is the DDL enveloping the clay mineral surfaces in the calculation with the MC approach.

The effect of anion exclusion reduces uranium migration in the MC diffusion approach. In our simulations, the anionic complex $CaUO_2(CO_3)_3^{2-}$ is the predominant species in the porewater of the Opalinus Clay because of the geochemical system [11]. Due to the negatively charged surfaces of the clay minerals mainly cations are enriched in the respective DDL decreasing the accessible pore space for anionic species and thus reducing their diffusive transport [5,41,46]. For the MC_{4Clay} simulations, anion exclusion decreased uranium diffusion by about 0.02 m in the shaly and 0.07 m in the carbonate-rich facies corresponding to about 14% and 30% reduction compared to SC, respectively (Figure 3). Thus, for the shaly facies, our results contradict the estimate of Hennig et al. [11] that diffusion lengths are reduced by 30% due to anion exclusion. However, the estimate applies for the carbonate-rich facies. The accessible pore space directly depends on the ionic strength of the porewater with a decreasing thickness of the DDL with increasing ionic strength [36,41]. Therefore, anion exclusion and with it the deviation in migration lengths between the SC and MC approach are different in the shaly and carbonate-rich facies (Figure 3a–c). Due to the lower ionic strength in the carbonate-rich compared to the shaly facies, the DDL is about 0.1 nm thicker (Shaly-76 and Carb-rich, Table 1) and thus anion exclusion is stronger. Accordingly, the deviation between both approaches should be the greatest in the sandy facies with the thickest DDL (Table 1). However, in the case of the sandy facies, uranium migrates farther instead of less into the model for the MC_{4Clay} simulation compared to the SC (Figure 3d). Only for the MC_{2Clay} scenario the sandy facies compares with the others as uranium migration is also reduced by 0.08 m, equivalent to about 30%. Therefore, anion exclusion is only one of the effects that explains the deviation in migration lengths between the two approaches. For the shaly as well as carbonate-rich facies, uranium migration is overestimated using the SC approach due to anion exclusion. A general estimate, how strong anion exclusion reduces the diffusion

lengths cannot be made because of the dependence on the porewater chemistry. However, the reduced diffusion length due to anion exclusion determined here is an estimate for other clay formations with similar geochemistry and mineralogy.

Uranium mainly sorbs on illite and montmorillonite. The investigated model concepts, MC_{4Clay} and MC_{2Clay} , differ in their composition of clay minerals selected (Section 2.2). MC_{4Clay} is considered with the four clay minerals chlorite, kaolinite, illite and montmorillonite, whereas in the MC_{2Clay} model only the minerals illite and montmorillonite are taken into account for sorption. The K_d values calculated in PHREEQC and thus the sorption capacity of the individual facies (Table 3) decrease with the amount of illite and montmorillonite and hence the clay content in general (Table 1). Accordingly, the sample Shaly-76 has the highest sorption capacity followed by Shaly-61, sandy and carbonate-rich with the lowest (MC_{4Clay} , Table 3). Comparing the K_d values of both concepts (MC_{4Clay} and MC_{2Clay} , Table 3), it becomes clear that the contribution of chlorite and kaolinite to the uranium sorption is only about 10% in the carbonate-rich as well as in the shaly facies and about 30% in the sandy facies. Consequently, the majority of uranium is retained by illite and montmorillonite. From this point of view, one could say that illite and montmorillonite are sufficient to be considered to describe the sorption of uranium with a respective uncertainty for the shaly and carbonate-rich facies. However, this does not apply for the sandy facies as the contribution of chlorite and kaolinite to uranium sorption is in that case much larger with 30%. As already discussed by Hennig et al. [11], sorption in the sandy facies is only slightly larger than in the carbonate-rich due to the geochemistry of the porewater (e.g., pH and Ca^{2+} concentration), although in the sandy facies are about 20 wt.% more clay minerals present. This also applies to our calculated K_d values of both facies (Table 3) and indicates that the contribution of kaolinite and chlorite to uranium sorption in the sandy facies is increased due to the porewater composition. Thus, we can confirm the findings of Hennig et al. [11] on the facies-dependence of uranium sorption in the Opalinus Clay and the governing role of the porewater geochemistry on sorption processes.

Chlorite plays a geochemical key role for the diffusive uranium transport using the MC diffusion approach. Due to the determined point of zero charge (pzc) of 9.5 for the chlorite used here [47] and the corresponding SCM data for uranium [48], the mineral surface is positively charged in the pH range present in the facies of the Opalinus Clay as a result of the interaction between porewater and prevailing minerals for the applied pCO_2 [11]. This leads to an enrichment of anionic species, such as the predominant anionic, ternary uranyl complex, in the DDL to compensate the remaining net surface charge and thus the highest uranium concentrations could be observed in the DDL of chlorite. This in turn affects the migration behaviour of uranium as the accessible pore space is increased instead of decreased compared to the clay minerals with a negative surface charge. The contribution of chlorite to the total transport of uranium depends on the thickness of the DDL and thus on the ionic strength of the porewater. A lower ionic strength means a thicker DDL and in the case of the chlorite used here an enhanced diffusion of uranium instead of an intensified effect of anion exclusion as it would be the case for the clay minerals with negatively charged surfaces. Therefore, a farther uranium migration into the formation was observed in the sandy facies for the MC_{4Clay} simulation compared to SC and hence counteracts anion exclusion (Figure 3d). Without chlorite (MC_{2Clay} , Figure 3d), the anion exclusion effect is fully effective. This emphasizes the important role of chlorite within the system, especially for the migration of uranium or other anionic radionuclides such as selenite in the sandy facies. However, the thermodynamic data used here are based on investigations of an almost pure chlorite sample taken from a granite fracture in the rock laboratory Grimsel (Switzerland) [47,48]. It serves for us as an analogue, because chlorite from the Opalinus Clay has not yet been studied in detail. It therefore remains unclear, whether chlorite from Grimsel and Mont Terri actually correspond in their chemical properties. For instance, a $pzc < 7$ would result in a negatively charged surface for the geochemical conditions and turn around the behaviour of the system. In this case, the determined migration lengths would correspond to the MC_{2Clay} scenarios. Accordingly, a

detailed characterization of the clay minerals in the Opalinus Clay and of their individual properties is essential and indicates the need for further research.

The sulphate concentration in the porewater limits the contribution of chlorite to uranium migration. In addition to uranium, other anions from the porewater such as chloride or sulphate are also enriched in the DDL of chlorite to compensate the positively charged surface of the mineral. Chloride ions are mainly present in the DDL of illite, whereas for sulphate, similar to for uranium, the highest concentrations have been observed in the DDL of chlorite (Figure 4b). Due to the same negative charge of two, both anions compete with each other in the DDL. This was also determined by the concentrations along the x-axis. With decreasing uranium concentration in the DDL of chlorite, the sulphate concentration simultaneously increases (Figure 4c,d). Accordingly, a higher initial sulphate concentration in the porewater (Table 1) is associated with a potentially lower uranium concentration in the DDL of chlorite and thus less impact of chlorite on the diffusive uranium transport (Figure 3). This also explains the difference between the simulations MC_{4Clay} and MC_{2Clay} between the individual facies. Due to the higher initial concentrations of sulphate in the Shaly-76 and carbonate-rich facies (Table 1), chlorite does not contribute significantly to the uranium transport and so mineral selection only affects sorption (Figure 3a,b). On the contrary, the lower sulphate concentration in the porewaters for the sample Shaly-61 and of the sandy facies (Table 1) enable an enhanced uranium transport via the chlorite DDL (Figure 3c,d). Consequently, the chlorite DDL accelerates uranium migration only for low sulphate concentrations.

Besides sulphate, the concentrations of calcium and magnesium in the porewater are also decisive for the influence of the DDL on uranium migration. For instance, Wigger and Van Loon [36] observed in anion diffusion experiments that the negative surface charge was more strongly shielded at the same ionic strength by bivalent cations, such as calcium, compared to monovalent ones, such as sodium. Consequently, the anion exclusion effect is reduced by a higher concentration of bivalent cations [36]. In relation to our results, this means that the anion exclusion effect in the sandy facies is intensified by the lower concentrations of bivalent cations in the porewater compared to the other facies (Table 1) in addition to the thicker DDL. In that way, the geochemistry in the porewaters governs how strong the different DDL affect uranium migration. Thus, we confirm the findings of Hennig et al. [11] that the geochemistry is more decisive than the clay minerals. Furthermore, we can supplement that the geochemistry of the porewater not only controls sorption processes but also the diffusive transport of uranium in the Opalinus Clay. Our results also provide indications for the migration of uranium or other anionic radionuclides in clay formations with similar mineralogy and underline the importance of a detailed determination of the porewater and the geochemical system for each potential site.

5.2. Effect of Varying Mineralogy on Multi-Component Diffusion

The variation of the total mineral amount led to significant differences in the migration lengths. The assumptions inherent in the models regarding the hydro-physical parameters cause uncertainties in the results, since they determine the amount of rock per kg porewater and thus sorption as well as the accessible pore space. Therefore, we studied in minimum and maximum scenarios for the total amount of rock per kg porewater (Section 2.2) on the metre-scale the diffusion lengths.

The distribution coefficient K_d is unaffected by the variation in the total amount of minerals. In all facies, the K_d was the same for the minimum and maximum scenarios (MC_{max} and MC_{min} , Table 3), although the total amount of minerals differed by up to 6 kg per kg porewater within a facies (Table 2). The K_d indicates the ratio between sorbed and dissolved species for a defined mineral composition and porewater chemistry. As long as identical proportions of the individual clay minerals are used in the simulations, the total amount of minerals has no influence on the K_d . However, the total amount of sorbed uranium is affected by this and so is the diffusion length. In many sorption experiments, it has been observed, how strongly uranium sorption depends on the chemical properties

of the porewater, such as pH or carbonate concentration [31,49,50]. Furthermore, for the Opalinus Clay, we showed that the porewater chemistry is more decisive for the sorption of uranium than the quantity of clay minerals.

Changing amounts of minerals directly lead to changes in the amount of water in the DDL and in the pore space. For all facies, a farther uranium migration into the formation was observed for the minimum scenario (Figure 5). On the one hand, this is related to the reduced quantity of minerals available for sorption. However, as long as the porewater chemistry does not change, the sorption capacity is only slightly affected. On the other hand, the variation in migration for the investigated scenarios is much more affected due to changes of the total amount of water in the DDL with the mineral quantity. A smaller amount of minerals means, for instance, less water in the DDL of the negatively charged surfaces. Consequently, anion exclusion is attenuated and uranium migrates farther into the formation. This also applies for other clay formations. Furthermore, more pore space for diffusive transport in the minimal scenarios is available compared to the maximum scenario. Concerning the calibrated transport parameters K_d and D_e for the different scenarios (Table 3), it becomes clear that the total amount of minerals constrains transport within the facies. It is important to note that the averaged values of the hydro-physical parameters for the locations representing the sandy as well as carbonate-rich facies (Table 1) are very similar to the maximum values for the respective facies (Table 2), therefore the calculated diffusion lengths are also almost identical for the reference (MC_{4Clay}) and the maximum scenario (MC_{max}). Thus, the priority list for uranium sorption in the Opalinus Clay described by Hennig et al. [11] can also be confirmed for the migration and supplemented with the hydro-physical parameters as follows: pCO_2 , Ca^{2+} concentration, pH, pe, hydro-physical parameters and the amount of clay minerals.

5.3. Implications for the Host Rock Scale

We developed a workflow to set-up surrogate models on the metre-scale for efficient application on the host rock scale. As the previously investigated MC scenarios could be reproduced on the metre-scale with the SC approach using the calibrated K_d and D_e (Figures 3 and 5), the application to the host rock scale was evaluated by comparison with a representative MC simulation for each facies and for a simulation time of one million years (Figure 6). The MC_{4Clay} simulations could be reproduced on the host rock scale with the transport parameters calibrated on the small scale with a deviation between 2% and 4% (Figure 6).

Scale invariance enables the application of the calibrated K_d and D_e from the metre-scale to the host rock scale. The properties of a state and chemical processes remain largely or exactly the same and universality is given. Based on our presented modeling workflow, transport parameters for varying mineralogy and chemistry can therefore be determined. Since SC simulations using the calibrated transport parameters only required a few seconds (<10 s) of computing time, this represents time saving on the order of 10^4 for the host rock scale compared to full complexity MC simulations, which require up to 6 h (=21,600 s). This improvement enables performing 'MC' diffusion simulations on the host rock scale, for instance for a sequence of facies or in 2D models, with acceptable computing times and without numerous previous experiments otherwise required.

Uranium migration in Opalinus Clay is facies-dependent and its diffusion length is constrained by the rock type itself (shaly, sandy, carbonate-rich), as well as by the respective internal heterogeneity of varying mineral amounts and compositions. On the host rock scale, this results in an offset of up to 25 m between the shaly facies with a maximum amount of clays and the sandy facies with a minimum amount of clays (Figure 6a,d). Within the sandy facies for instance, variations in porosity and bulk densities led to a deviation between the diffusion lengths of up to 13 m (Figure 6d). In contrast, the diffusion lengths in the shaly facies varied by 5 m (Figure 6a) and in the carbonate-rich one even only by 2 m (Figure 6b). Due to the high amount of clay minerals in the shaly facies, heterogeneities are buffered, whereas in the carbonate-rich variations in the hydro-physical parameters are less

effective because of the low clay content in combination with the porewater composition. In the case of the sandy facies, the heterogeneity within the individual facies causes a higher uncertainty regarding the diffusion lengths compared to the shaly and carbonate-rich. Our simulation results demonstrate the effect of hydro-physical parameters and the amount of clay minerals on migration, especially on the transport properties. This influence of heterogeneity on transport properties does not only apply to the Opalinus Clay, but it is likely that this is also the case for any other clay formation. In any case, detailed measurements are required because facies or clay formations in general can vary immensely in their properties on the dm-scale, e.g., for the Opalinus Clay through clay layers within the sandy facies and vice versa [51]. It is shown for the sandy facies, compared the shaly and carbonate-rich ones, that, with decreasing clay content within the rock, the variation in mineral composition and its effect on the porewater chemistry and with that on the transport behaviour of uranium increases.

On the host rock scale, it becomes obvious that the shaly facies is best suited for the storage of nuclear waste followed by the carbonate-rich and sandy ones due to the shorter diffusion lengths. The high amount of clay minerals in the shaly facies (>50%) dominates diffusion and sorption processes and hence better compensates chemical and mineralogical heterogeneities compared to the other facies, which is apparent from the shorter diffusion lengths and their smaller span. This also means that the SC approach is sufficient for the shaly as well as carbonate-rich facies, since the deviation in the diffusion lengths for the two approaches but also by the mineralogical heterogeneity itself is negligible. However, the use of the SC approach for the sandy facies results in an over- or underestimation of maximum diffusion length and hence implies a high degree of uncertainty, especially due to the mineralogical heterogeneity. Nevertheless, uranium is still retained in any case within the effective containment zone of a potential host rock with a thickness of 100 m and hence the Opalinus Clay fulfills the minimum requirements for a potential storage site (§22 Article 5 StandAG).

Due to the decisive role of the porewater geochemistry in the system, the diffusion lengths determined here cannot be directly transferred to other sites. However, the insights on the MC diffusion of uranium in clay formations gained here, e.g., the role of the chlorite DDL and the sulphate concentration, can be taken as directions for future works and other sites since uranium is one of the most important radionuclides for the long-term safety of a potential repository. The modular structure of our concept (porewater composition and mineralogy) offers the opportunity to use this workflow for other potential sites or radionuclides, if all data are available.

6. Conclusions and Outlook

The significance of multi-component (MC) compared to single-component (SC) diffusion approaches was shown within one-dimensional simulations on the metre as well as on the host rock scale for uranium transport and sorption in Opalinus Clay depending on varying mineralogy and porewater geochemistry. The MC approach enables a process-based description of diffusive transport as it takes into account the interaction of the involved chemical species with the diffuse double layers (DDL) adhering the clay mineral surfaces. Due to the huge computational effort of MC diffusion simulations on the host rock scale, a surrogate model based on a distribution coefficient K_d (m^3/kg) and an effective diffusion coefficient D_e (m^2/s) was developed with a workflow to calibrate the parameters on the metre-scale and transfer them as pseudo-MC diffusion to larger scales.

The three facies, shaly, sandy and carbonate-rich, were represented by analyses from boreholes at the underground research laboratory Mont Terri in Switzerland. Porewater geochemistry was controlled by a constant partial pressure of carbon dioxide ($p\text{CO}_2$) and mineral equilibria with the carbonates dolomite and calcite as well as siderite and pyrite. The resulting porewater chemistry is facies-dependent and varies with the individual mineral assemblage significantly affecting sorption as well as the diffusive transport.

In the MC diffusion approach implemented in PHREEQC, diffusion coefficients are determined analogous to Archie's law and hence the medium specific parameter n had to be calibrated for our model. We did this successfully by means of a diffusion experiment with Opalinus Clay and uranium [17]. Based on a bottom-up approach, surface complexation and cation exchange are used to implement sorption processes.

A high clay content (>50 wt.%), such as in the shaly facies of the Opalinus Clay, dominates diffusion and sorption processes of uranium with short migration lengths of 10 to 19 m within one million years depending on their heterogeneity. The MC simulations show shorter diffusion lengths than the SC models, but the differences with less than one metre are almost neglectable. For the carbonate-rich facies, diffusion lengths are 16 m to 18 m using the MC approach with 7 m difference between MC and SC. The simplified SC model overestimates the diffusion length of uranium. For the sandy facies, it depends on the selected mineral composition, if the MC under- or overestimates the SC simulations by 8 m or 2 m, respectively. The migration length ranges between 16 m and 35 m. Considering the clay minerals illite, montmorillonite, chlorite and kaolinite for sorption, the calculated K_d values ranged between $0.004 \text{ m}^3/\text{kg}$ for Shaly-76 with the highest clay mineral content and $0.0014 \text{ m}^3/\text{kg}$ for the carbonate-rich with the lowest. The K_d of the sandy facies with a value of $0.0016 \text{ m}^3/\text{kg}$ is only slightly higher despite the 20 wt.% more clay minerals compared to the carbonate-rich highlighting the increasing influence of geochemistry on sorption with decreasing amount of clay minerals.

Variations in migration of uranium in the MC approach can be attributed to the different porewater compositions in the facies in combination with the DDL on the clay mineral surfaces. A high ionic strength reduces the thickness of the DDL and thus the accessible pore space for diffusion is increased. Further, the porewater geochemistry interacts with the charged mineral surfaces. Negatively charged surfaces attract cations and exclude anions to or from the DDL. This is known as anion exclusion effect. The accessible pore space is reduced and the migration of the anions is hampered. This is the reason the MC simulations show shorter diffusion lengths of up to 30% compared to the SC models. A higher concentration of bivalent cations in the porewater shields the negative surface charge of the clay minerals better and hence decreases anion exclusion. The latter is the case within the shaly facies of the Opalinus Clay and reduces the effect of anion exclusion. This, in combination with a higher ionic strength, reduces the diffusion length in the shaly facies by 14% compared to SC. Conversely, positively charged mineral surfaces attract anions. This is the case for chlorite for the studied geochemical system of the Opalinus Clay as it attracts, e.g., the predominant uranium species $\text{CaUO}_2(\text{CO}_3)_3^{2-}$. This means an increased accessible pore space for uranium enhancing the diffusive transport compared to the other clay minerals illite, montmorillonite and kaolinite with negatively charged surfaces. This is the reason, why simulations for the sandy facies show increased diffusion lengths for MC compared to SC models. As anion with the same negative charge, sulphate competes with the anionic, ternary uranyl complex in the DDL of chlorite. Therefore, a higher sulphate concentration in the pore water reduces the enhancing influence of chlorite on the uranium transport as can be seen for the shaly and carbonate-rich facies.

Hydro-physical parameters, such as porosity or bulk densities, have an impact on the diffusion lengths as assessed in scenarios with varying total amounts of rock per kg porewater. These parameters determine the ratio between rock and porewater within the pore space and thus control the amount of water in the DDL. Uranium migration can be significantly enhanced by the variation in hydro-physical rock properties in combination with an appropriate composition of the porewater, i.e., a low concentration of sulphate and bivalent cations. Calibrated D_e for uranium varied for the facies between $8 \times 10^{-13} \text{ m}^2/\text{s}$ and $4.5 \times 10^{-12} \text{ m}^2/\text{s}$. Therefore, uranium diffusion and sorption in the Opalinus Clay is governed in descending priority by pCO_2 , Ca^{2+} concentration, pH, pe, the hydro-physical parameters and the amount of clay minerals.

Due to the high computational costs of MC diffusion simulations, they are inefficient for larger and more complex models such as on the host rock scale. Therefore, we developed

a surrogate. Based on the results of the MC simulations on the metre-scale, we determined K_d and D_e and showed that they can successfully be applied to the host rock scale and required simulation times up to one million years. In that way, we achieved a time saving on the order of 10^4 . Consequently, a detailed description of porewater chemistry and hydro-physical properties from field or laboratory studies in combination with our workflow using MC diffusion simulations is a powerful tool to quantify uranium migration on the host rock scale for varying mineralogy and geochemistry of potential repository sites in other clay formations. Our workflow offers the possibility for pseudo-MC diffusion simulations applied for complex 2D as well as 3D models accounting for anisotropy and heterogeneity of facies, which will be required in performance assessments of a repository. Further, with the help of our approach, the design of diffusion experiments can be assisted. After a simulation time of one million years, the maximum determined diffusion length of uranium was 35 m in the sandy facies. With respect to the minimum requirement of a thickness of 100 m, the Opalinus Clay seems to be a suitable host rock, as it effectively retains the radionuclide and no adjacent aquifer is reached.

Supplementary Materials: The following are available at <https://www.mdpi.com/2076-3417/11/2/786/s1>.

Author Contributions: Conceptualization, T.H. and M.K.; software, T.H.; investigation, T.H.; writing—original draft preparation, T.H.; writing—review and editing, T.H. and M.K.; supervision, M.K.; and funding acquisition, M.K. All authors have read and agreed to the published version of the manuscript.

Funding: This research was funded by the German Federal Ministry of Education and Research (project number 02NUK053D), the Helmholtz Association (project number SO-093) and the GFZ German Research Centre for Geosciences Potsdam.

Institutional Review Board Statement: Not applicable.

Informed Consent Statement: Not applicable.

Data Availability Statement: Data is contained within the article and supplementary material.

Conflicts of Interest: The authors declare that they have no known competing financial interests or personal relationships that could have appeared to influence the work reported in this paper.

Abbreviations

The following abbreviations are used in this manuscript:

DDL	Diffuse double layer
D_e	Effective diffusion coefficient (m^2/s)
D_p	Pore diffusion coefficient (m^2/s)
D_w	Self-diffusion coefficient in water (m^2/s)
ϵ	Porosity (-)
K_d	Distribution coefficient (kg/m^3)
MC	Multi-component
n	medium-specific, empirical exponent in Archie's law (-)
pCO ₂	Partial pressure of carbon dioxide (bar)
pzc	point of zero charge
rRMSE	Relative root mean square error (-)
SC	Single-component
SCM	Surface complexation model

References

1. IAEA. *Scientific and Technical Basis for the Geological Disposal of Radioactive Wastes*; Technical Report; International Atomic Energy Agency: Vienna, Austria, 2003.
2. Nagra. *Project Opalinus Clay—Safety Report*; Nagra Technical Report; NTB 02-05; Nagra: Wettingen, Switzerland, 2002.
3. Delay, J.; Rebours, H.; Vinsot, A.; Robin, P. Scientific investigation in deep wells for nuclear waste disposal studies at the Meuse/Haute Marne underground research laboratory, Northeastern France. *Phys. Chem. Earth* **2007**, *32*, 42–57. [[CrossRef](#)]

4. Mazurek, M.; Gautschi, A.; Marschall, P.; Vigneron, G.; Lebon, P.; Delay, J. Transferability of geoscientific information from various sources (study sites, underground rock laboratories, natural analogues) to support safety cases for radioactive waste repositories in argillaceous formations. *Phys. Chem. Earth* **2008**, *33*, S95–S105. [[CrossRef](#)]
5. Appelo, C.A.J.; Wersin, P. Multicomponent diffusion modeling in clay systems with application to the diffusion of tritium, iodide, and sodium in opalinus clay. *Environ. Sci. Technol.* **2007**, *41*, 5002–5007. [[CrossRef](#)] [[PubMed](#)]
6. Appelo, C.A.J.; Van Loon, L.R.; Wersin, P. Multicomponent diffusion of a suite of tracers (HTO, Cl, Br, I, Na, Sr, Cs) in a single sample of Opalinus Clay. *Geochim. Cosmochim. Acta* **2010**, *74*, 1201–1219. [[CrossRef](#)]
7. Tournassat, C.; Bourg, I.C.; Steefel, C.I.; Bergaya, F. Surface Properties of Clay Minerals. *Dev. Clay Sci.* **2015**, *6*, 5–31. [[CrossRef](#)]
8. Altmann, S. 'Geo'chemical research: A key building block for nuclear waste disposal safety cases. *J. Contam. Hydrol.* **2008**, *102*, 174–179. [[CrossRef](#)]
9. Bossart, P.; Bernier, F.; Birkholzer, J.; Bruggeman, C.; Connolly, P.; Dewonck, S.; Fukaya, M.; Herfort, M.; Jensen, M.; Matray, J.M.; et al. Mont Terri rock laboratory, 20 years of research: introduction, site characteristics and overview of experiments. *Swiss J. Geosci.* **2017**, *110*, 3–22. [[CrossRef](#)]
10. Pearson, F.J.; Arcos, D.; Bath, A.; Boisson, J.Y.; Fernández, A.M.; Gäbler, H.E.; Gaucher, E.C.; Gautschi, A.; Griffault, L.; Hernán, P.; et al. *Mont Terri Project—Geochemistry of Water in the Opalinus Clay Formation at the Mont Terri Rock Laboratory*; Technical Report 5; Federal Office for Water and Geology (FOWG): Bern, Switzerland, 2003.
11. Hennig, T.; Stockmann, M.; Kühn, M. Simulation of diffusive uranium transport and sorption processes in the Opalinus Clay. *Appl. Geochem.* **2020**, *123*. [[CrossRef](#)]
12. Metz, V.; Geckeis, H.; González-Robles, E.; Loida, A.; Bube, C.; Kienzler, B. Radionuclide behaviour in the near-field of a geological repository for spent nuclear fuel. *Radiochim. Acta* **2012**, *100*, 699–713. [[CrossRef](#)]
13. Parkhurst, D.L.; Appelo, C.A.J. Description of input and examples for PHREEQC Version 3—A computer program for speciation, batch-reaction, one-dimensional transport, and inverse geochemical calculations. In *U.S. Geological Survey Techniques and Methods*; U.S. Geological Survey: Denver, CO, USA, 2013; Volume Book 6, Chapter A43, p. 497.
14. Kerisit, S.; Liu, C. Molecular simulation of the diffusion of uranyl carbonate species in aqueous solution. *Geochim. Cosmochim. Acta* **2010**, *74*, 4937–4952. [[CrossRef](#)]
15. Liu, C.; Shang, J.; Zachara, J.M. Multispecies diffusion models: A study of uranyl species diffusion. *Water Resour. Res.* **2011**, *47*, 1–16. [[CrossRef](#)]
16. Wersin, P.; Mazurek, M.; Mäder, U.K.; Gimmi, T.; Rufer, D.; Lerouge, C.; Traber, D. Constraining porewater chemistry in a 250 m thick argillaceous rock sequence. *Chem. Geol.* **2016**, *434*, 43–61. [[CrossRef](#)]
17. Joseph, C.; Van Loon, L.R.; Jakob, A.; Steudtner, R.; Schmeide, K.; Sachs, S.; Bernhard, G. Diffusion of U(VI) in Opalinus Clay: Influence of temperature and humic acid. *Geochim. Cosmochim. Acta* **2013**, *109*, 74–89. [[CrossRef](#)]
18. Keesmann, S.; Noseck, U.; Buhmann, D.; Fein, E.; Schneider, A. *Modellrechnungen zur Langzeitsicherheit von Endlagern in Salz- und Granitformationen*; Technical Report GRS-206; Gesellschaft für Anlagen- und Reaktorsicherheit (GRS) mbH: Köln, Germany, 2005.
19. Wersin, P.; Gaucher, E.C.; Gimmi, T.; Leupin, O.X.; Mäder, U.K.; Pearson, F.J.; Thoenen, T.; Tournassat, C. *Geochemistry of Porewaters in Opalinus Clay at Mont Terri: Experimental Data and Modelling*; Mont Terri Project, Technical Report; TR 2008-06; Mont Terri Project: St. Ursanne, Switzerland, 2009.
20. Bradbury, M.H.; Baeyens, B. *Derivation of In-Situ Opalinus Clay Porewater Compositions from Experimental and Geochemical Modelling Studies*; Nagra Technical Report, NTB 97-07; Nagra: Wetztingen, Switzerland, 1997.
21. Pearson, F.J.; Tournassat, C.; Gaucher, E.C. Biogeochemical processes in a clay formation in situ experiment: Part E—Equilibrium controls on chemistry of pore water from the Opalinus Clay, Mont Terri underground research laboratory, Switzerland. *Appl. Geochem.* **2011**, *26*, 990–1008. [[CrossRef](#)]
22. Vinsot, A.; Appelo, C.A.J.; Cailteau, C.; Wechner, S.; Pironon, J.; De Donato, P.; De Cannière, P.; Mettler, S.; Wersin, P.; Gäbler, H.E. CO₂ data on gas and pore water sampled in situ in the Opalinus Clay at the Mont Terri rock laboratory. *Phys. Chem. Earth* **2008**, *33*, 54–60. [[CrossRef](#)]
23. Wersin, P.; Leupin, O.X.; Mettler, S.; Gaucher, E.C.; Mäder, U.; De Cannière, P.; Vinsot, A.; Gäbler, H.E.; Kunimaro, T.; Kiho, K.; et al. Biogeochemical processes in a clay formation in situ experiment: Part A—Overview, experimental design and water data of an experiment in the Opalinus Clay at the Mont Terri underground research laboratory, Switzerland. *Appl. Geochem.* **2011**, *26*, 931–953. [[CrossRef](#)]
24. Lerouge, C.; Blessing, M.; Flehoc, C.; Gaucher, E.C.; Henry, B.; Lassin, A.; Marty, N.; Matray, J.; Proust, E.; Rufer, D.; et al. Dissolved CO₂ and alkane gas in clay formations. *Procedia Earth Planet. Sci.* **2015**, *13*, 88–91. [[CrossRef](#)]
25. Gaucher, E.C.; Lassin, A.; Lerouge, C.; Fléhoc, C.; Marty, N.C.M.; Benoit, H.; Tournassat, C.; Altmann, S.; Vinsot, A.; Buschaert, S. *CO₂ Partial Pressure in Clayrocks: A General Model*; Water-Rock Interaction WRI-13; HAL (archive hal-00664967): Guanajuato, Mexico, 2010; pp. 855–858.
26. Bossart, P.; Thury, M. *Characteristics of the Opalinus Clay at Mont Terri*; Reports of the Swiss Geological Survey, No. 3; Swiss Geological Survey: Wabern, Switzerland, 2008.
27. Marques Fernandes, M.; Vér, N.; Baeyens, B. Predicting the uptake of Cs, Co, Ni, Eu, Th and U on argillaceous rocks using sorption models for illite. *Appl. Geochem.* **2015**, *59*, 189–199. [[CrossRef](#)]

28. Stockmann, M.; Schikora, J.; Becker, D.A.; Flügge, J.; Noseck, U.; Brendler, V. Smart Kd-values, their uncertainties and sensitivities—Applying a new approach for realistic distribution coefficients in geochemical modeling of complex systems. *Chemosphere* **2017**, *187*, 277–285. [[CrossRef](#)]
29. Dzombak, D.A.; Morel, F.M.M. *Surface Complexation Modeling: Hydrous Ferric Oxide*; Jon Wiley and Sons: New York, NY, USA, 1990; p. 393.
30. Hyun, S.P.; Cho, Y.H.; Hahn, P.S.; Kim, S.J. Sorption mechanism of U(VI) on a reference montmorillonite: Binding to the internal and external surfaces. *J. Radioanal. Nucl. Chem.* **2001**, *250*, 55–62. [[CrossRef](#)]
31. Joseph, C.; Stockmann, M.; Schmeide, K.; Sachs, S.; Brendler, V.; Bernhard, G. Sorption of U(VI) onto Opalinus Clay: Effects of pH and humic acid. *Appl. Geochem.* **2013**, *36*, 104–117. [[CrossRef](#)]
32. Bradbury, M.H.; Baeyens, B. Modelling the sorption of Mn(II), Co(II), Ni(II), Zn(II), Cd(II), Eu(III), Am(III), Sn(IV), Th(IV), Np(V) and U(VI) on montmorillonite: Linear free energy relationships and estimates of surface binding constants for some selected heavy metals and actinide. *Geochim. Cosmochim. Acta* **2005**, *69*, 875–892. [[CrossRef](#)]
33. Bradbury, M.H.; Baeyens, B.; Geckeis, H.; Rabung, T. Sorption of Eu(III)/Cm(III) on Ca-montmorillonite and Na-illite. Part 2: Surface complexation modelling. *Geochim. Cosmochim. Acta* **2005**, *69*, 5403–5412. [[CrossRef](#)]
34. Bradbury, M.H.; Baeyens, B. *Experimental and Modelling Investigations on Na-Illite: Acid-Base Behaviour and the Sorption of Strontium, Nickel, Europium and Uranyl*; Nagra Technical Report, NTB 04-02; Nagra: Wettingen, Switzerland, 2005.
35. Hartmann, E.; Geckeis, H.; Rabung, T.; Lützenkirchen, J.; Fanghänel, T. Sorption of radionuclides onto natural clay rocks. *Radiochim. Acta* **2008**, *96*, 699–707. [[CrossRef](#)]
36. Wigger, C.; Van Loon, L.R. Effect of the pore water composition on the diffusive anion transport in argillaceous, low permeability sedimentary rocks. *J. Contam. Hydrol.* **2018**, *213*, 40–48. [[CrossRef](#)]
37. Appelo, C.A.J.; Vinsot, A.; Mettler, S.; Wechner, S. Obtaining the porewater composition of a clay rock by modeling the in- and out-diffusion of anions and cations from an in-situ experiment. *J. Contam. Hydrol.* **2008**, *101*, 67–76. [[CrossRef](#)]
38. Appelo, C.A.J. Multicomponent diffusion in clays. In *Water Pollution in Natural Porous Media*; Instituto Geologica de Espana: Madrid, Spain, 2007; Volume 1, pp. 3–13. [[CrossRef](#)]
39. Appelo, C.A.J. Solute transport solved with the Nernst-Planck equation for concrete pores with ‘free’ water and a double layer. *Cem. Concr. Res.* **2017**, *101*, 102–113. [[CrossRef](#)]
40. Gratwohl, P. *Diffusion in Natural Porous Media: Contaminant Transport, Sorption/Desorption and Dissolution Kinetics*; Kluwer Academic Publishers: London, UK, 1958.
41. Van Loon, L.R.; Glaus, M.A.; Müller, W. Anion exclusion effects in compacted bentonites: Towards a better understanding of anion diffusion. *Appl. Geochem.* **2007**, *22*, 2536–2552. [[CrossRef](#)]
42. Van Loon, L.R.; Leupin, O.X.; Cloet, V. The diffusion of SO₄²⁻ in Opalinus Clay: Measurements of effective diffusion coefficients and evaluation of their importance in view of microbial mediated reactions in the near field of radioactive waste repositories. *Appl. Geochem.* **2018**, *95*, 19–24. [[CrossRef](#)]
43. Van Loon, L.R.; Soler, J.M.; Jakob, A.; Bradbury, M.H. Effect of confining pressure on the diffusion of HTO, ³⁶Cl⁻ and ¹²⁵I⁻ in a layered argillaceous rock (Opalinus Clay): Diffusion perpendicular to the fabric. *Appl. Geochem.* **2003**, *18*, 1653–1662. [[CrossRef](#)]
44. Mazurek, M.; Alt-Epping, P.; Bath, A.; Gimmi, T.; Waber, H. *Natural Tracer Profiles Across Argillaceous Formations: The CLAYTRAC Project*; Technical Report; Nuclear Energy Agency and Organisation for Economic Co-Operation and Development: Paris, France, 2009.
45. Van Loon, L.R.; Mibus, J. A modified version of Archie’s law to estimate effective diffusion coefficients of radionuclides in argillaceous rocks and its application in safety analysis studies. *Appl. Geochem.* **2015**, *59*, 85–94. [[CrossRef](#)]
46. Van Loon, L.R.; Soler, J.M.; Bradbury, M.H. Diffusion of HTO, ³⁶Cl⁻ and ¹²⁵I⁻ in Opalinus Clay samples from Mont Terri: Effect of confining pressure. *J. Contam. Hydrol.* **2003**, *61*, 73–83. [[CrossRef](#)]
47. Zorn, T. Untersuchungen der Sorption von Uran(VI) an das Gestein Phyllit zur Bestimmung von Oberflächenkomplexierungskonstanten. Ph.D. Thesis, Technische Universität Dresden, Dresden, Germany, 2000.
48. Arnold, T.; Zorn, T.; Zänker, H.; Bernhard, G.; Nitsche, H. Sorption behavior of U(VI) on phyllite: Experiments and modeling. *J. Contam. Hydrol.* **2001**, *47*, 219–231. [[CrossRef](#)]
49. Tournassat, C.; Tinnacher, R.M.; Grangeon, S.; Davis, J.A. Modeling uranium(VI) adsorption onto montmorillonite under varying carbonate concentrations: A surface complexation model accounting for the spillover effect on surface potential. *Geochim. Cosmochim. Acta* **2018**, *220*, 291–308. [[CrossRef](#)]
50. Philipp, T.; Shams Aldin Azzam, S.; Rossberg, A.; Huittinen, N.; Schmeide, K.; Stumpf, T. U(VI) sorption on Ca-bentonite at (hyper)alkaline conditions – Spectroscopic investigations of retention mechanisms. *Sci. Total. Environ.* **2019**, *676*, 469–481. [[CrossRef](#)] [[PubMed](#)]
51. Lauper, B.; Jaeggi, D.; Deplazes, G.; Foubert, A. Multi-proxy facies analysis of the Opalinus Clay and depositional implications (Mont Terri rock laboratory, Switzerland). *Swiss J. Geosci.* **2018**, *111*, 383–398. [[CrossRef](#)]